

U.S. National Standards for High Pressure Natural Gas Flow Measurement

Aaron N. Johnson

**National Institute of Standards and
Technology (NIST)**

100 Bureau Drive

Gaithersburg, MD 20899

301-975-5954

Aaron.Johnson@nist.gov

Bill Johansen

**Colorado Experimental
Engineering Station
Incorporated (CEESI)**

54043 County Rd. 37

Nunn, CO 80648

970-897-8207

BJohansen@ceesi.com

Abstract – NIST plans to establish a calibration service for flow meters used in the custody transfer of high pressure natural gas. These calibrations will provide internationally recognized flow traceability for the U.S. natural gas industry over a flow range from 0.25 m³/s (3.2 × 10⁴ acfh) to 9 m³/s (1.1 × 10⁶ acfh) at a nominal pressure of 7500 kPa and at ambient temperatures. Flow meter calibrations will be performed at CEESI's Iowa facility under NIST's metrological control, using working standards that are traceable to NIST's primary flow standards. The measurement uncertainty of these calibrations range from 0.25 % to 0.27 % (with a 95 % confidence level) depending on flow rate. This manuscript documents the five-stage scale-up process used to establish traceability between NIST's low-pressure, air-flow primary standard to flowmeters calibrated at CEESI's Iowa facility in natural gas at up to 54 times the volumetric flow and 10 times the pressure.

INTRODUCTION

NIST plans to establish a high pressure Natural Gas Flow Calibration Service (NGFCS) to provide internationally recognized flow traceability for the natural gas flowmetering community. When completed this calibration service will promote equitable custody transfer of natural gas within the U.S. and internationally.

NIST does not have a natural gas flow facility, but intends to extend its flow measurement standards and dissemination capabilities to natural gas flows at commercial pipeline conditions. To accomplish this objective, NIST has established contractual arrangements with natural gas flow facilities having the necessary capabilities. The combination of such contractual arrangements and the scale up of existing NIST capabilities is the basis for new NIST capability in natural gas flow meter calibrations and standards. A key aspect of this capability is that NIST extends and maintains metrological control of the calibration process while utilizing facilities not its own. NIST will ensure the accuracy and metrological control of this standards dissemination effort using the following approach:

1. establish a path of traceability linking the calibration of a meter under test (MUT) at an offsite flow facility to NIST primary flow standards,
2. extend the NIST quality system, compliant with ISO 17025 [1], to these calibration activities,
3. monitor each calibration procedure via a secure internet connection,
4. provide and maintain transfer standards to calibrate all auxiliary instrumentation required for calibrations (pressure transducers, temperature sensors, frequency counters, etc.),
5. maintain control charts to validate the performance of auxiliary instrumentation,
6. automate to the extent possible the calibration process
7. develop diagnostics to quantify flow stability levels, line pack (or mass storage) effects, the impact of changing environmental conditions, and other parameters affecting calibration results,

8. validate the results of each calibration using a check standard installed in series with the meter under tests (MUT),
9. analyze the raw calibration data, produce the results, and write the calibration report, and
10. participate in international key comparisons to detect potential biases in calibration results within the framework of the CIPM Mutual Recognition Arrangement.

This manuscript presents the results of implementing step 1 (*i.e.*, establishing flow traceability) for a particular offsite flow facility (Colorado Engineering Experimental Station Incorporated or CEESI). A five stage procedure is used to link calibrations done at CEESI's Iowa facility to NIST's 26 m³ primary flow standard. The intermediate stages of this process are used to bootstrap from the lower pressures and flows provided by NIST standards to pressures and flows realized for the custody transfer of natural gas in large pipelines.

The flow range of the NGFCS extends from 0.25 m³/s (3.2×10^4 acfh) to 9 m³/s (1.1×10^6 acfh) at a nominal pressure of 7500 kPa and at ambient temperatures. The expanded uncertainty (*i.e.*, $k = 2$) ranges from 0.25 % to 0.27 % with larger uncertainties corresponding to lower flows. Work is underway to reduce the uncertainty to 0.2 % while simultaneously extending the flow range down to 0.1 m³/s. The remainder of the manuscript describes the CEESI Iowa facility, explains the five stage process that NIST and CEESI have used to establish traceability, and gives the calibration results and the corresponding uncertainty of each stage.

DESCRIPTION OF CEESI's IOWA FLOW FACILITY

The CEESI Iowa flow facility is located adjacent to a pipeline transmission company that transports dry pipeline quality natural gas throughout the northwest region of the United States. Figure 1 shows a junction of the natural gas transmission pipeline used for custody transfer. Flow enters the custody transfer station on pipeline A at a nominal pressure of 7500 kPa and at ambient temperatures. The flow on pipeline A is divided into three separate pipelines labeled B, C, and D, before being delivered to its intended destination.

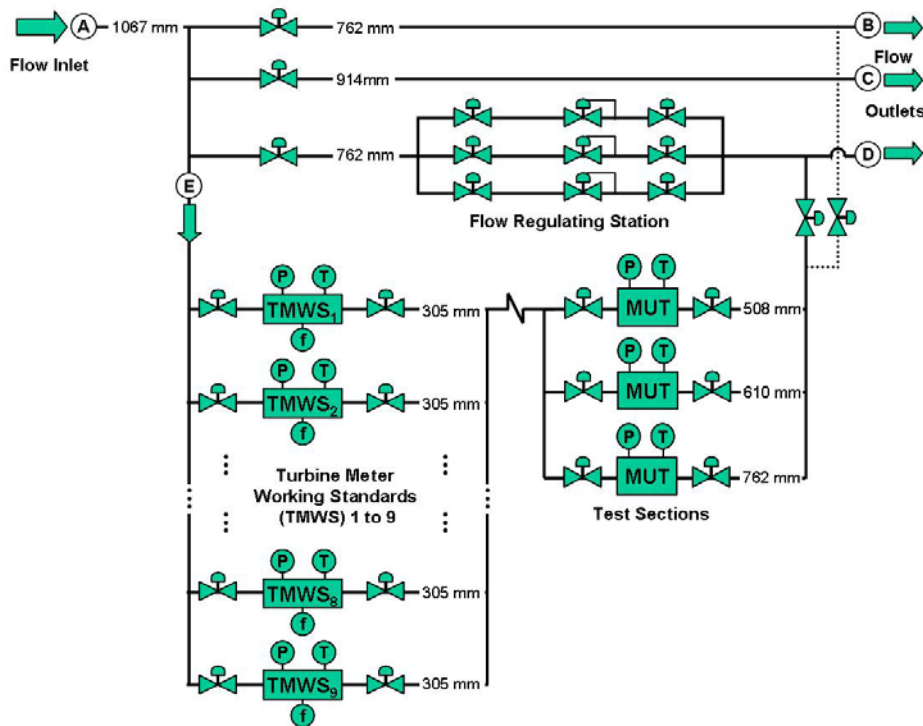


Figure 1. CEESI Iowa Natural Gas Flowmetering Facility

The CEESI Iowa flow facility was built at the custody transfer station along pipeline E as shown in Fig. 1. During a calibration, natural gas diverted from pipeline A to E is measured by a parallel array of up to nine turbine meter working standards (TMWS). The flowmeters being calibrated (or MUTs) are installed downstream in any one of three differently sized test sections. Conservation of mass is used to relate the volumetric flow at the MUT to the flow at the TMWS. After calibration, the flow exiting the MUT is returned to the pipeline company to be distributed to its intended destination.

OVERVIEW OF THE FIVE STAGE PROCESS USED TO ESTABLISH FLOW TRACEABILITY TO NIST

The five stage process scales up the pressure and flow of calibrations done using NIST's low pressure air-flow standard, thereby enabling NIST traceable calibrations of high pressure natural gas flows. A diagram of the five stage process is shown in Fig. 2. The first column in each row identifies the calibration stage, followed by the flow standard, the reference flowmeter being calibrated, the fluid medium, the expanded uncertainty (*i.e.*, $k = 2$) of the reference flowmeter, and the calibrated flow (or Reynolds number) range of the reference flowmeter. The nominal pressure conditions for all five stages are also specified in the figure.

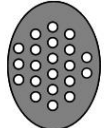
Stage	Flow Standard	Reference Flowmeter	Working Fluid	Expanded Unc. ($k = 2$) of Reference Flowmeter	Flow or Reynolds Number Range of Reference Flowmeter
1	NIST Flow Standard 	LP CFVs 4 x  $P_0 \approx 350$ to 700 kPa	air	0.10 %	LP CFV Re Range 1.1×10^6 to 2.4×10^6
2	LP Nozzle Bank  $P_0 \approx 350$ to 700 kPa	MP CFVs (Upstream of LP CFVs) 4 x  $4x P_0$	air	0.13 %	MP CFV Re Range 3.7×10^6 to 8.6×10^6
3	MP Nozzle Bank  $4x P_0$	HP CFVs (Upstream of MP CFVs) 8 x  $16x P_0$	air	0.17 %	HP CFV Re Range (dry air) 20×10^6 to 27.5×10^6
4	HP Nozzle Bank  $P_0 \approx 7500$ kPa	TMWS (Upstream of HP CFVs) 9 x  $P \approx 7500$ kPa	Natural Gas	0.24 % to 0.25 %	HP CFV Re Range (natural gas) 24×10^6 to 27.5×10^6
5	TMWS Array 9 x  $P \approx 7500$ kPa	MUT (Downstream of TMS)  $P \approx 7500$ kPa	Natural Gas	0.25 % to 0.27 %	TMWS Flow Range $0.25 \text{ m}^3/\text{s}$ to $9.0 \text{ m}^3/\text{s}$ ($P \approx 7500 \text{ kPa}$ and $T \approx \text{ambient}$)

Figure 2. Schematic of the five stage process used to establish traceability of a MUT at CEESI's Iowa natural gas flow facility to NIST 26 m³ PVTt primary flow standard.

A total of sixteen critical flow venturis (CFVs) and nine TMWS, are used to establish traceability between NIST's flow standards and a meter under test (MUT) at the Iowa flow facility. All of the CFVs have the same nominal throat diameter of $d = 2.54$ cm, and their geometry complies with the ISO 9300 toroidal throat design [2]. The sixteen CFVs are herein divided into three groupings based on their calibrated

pressure ranges. These three groupings are: 1) four low pressure (LP) CFVs calibrated in air over pressures from 350 kPa to 700 kPa; 2) four medium pressure (MP) CFVs calibrated in air over pressures from 1400 kPa to 2800 kPa; and 3) eight high pressure (HP) CFVs calibrated in air over pressures from 5600 kPa to 10 000 kPa. Each of the eight HP CFVs have sixteen times the pressure and flow capacity of the NIST flow standard to which they are traceable. After calibrating each of the TMWS against the eight HP CFVs, the nine TMWS are combined in parallel to calibrate a MUT in natural gas at volumetric flow capacities up to 54 times those of the NIST flow standard and pressures up to 10 times those of the NIST flow standard.

The five stage process begins by calibrating each of the four LP CFVs in air against the NIST 26 m³ PVTt flow standard [3]. Figure 3A shows the single aperture nozzle fixture used to hold each LP CFV during calibration, and Fig. 3B shows the four LP CFVs with their end caps. In Stage 2, the four LP CFVs are combined in parallel and used to calibrate each of the four MP CFVs in air. In this way, each of the MP CFVs is calibrated at four times the flow and pressure of the LP CFVs in Stage 1. Stage 3 is analogous to Stage 2. In Stage 3, the four MP CFVs are used in parallel to sequentially calibrate each of the eight HP CFVs in air at sixteen times the Stage 1 flow and pressure. Figure 3C shows the nozzle fixture used to hold the four LP CFVs in Stage 2 and the four MP CFVs in Stage 3. In Stage 4 the nozzle fixture with twenty-one apertures shown in Fig. 3D is used to house the eight HP CFVs. Only eight HP CFVs are needed to achieve the full scale of each TMWS so that the additional apertures in the nozzle fixture are not used (*i.e.*, the unused apertures are leak-checked and sealed during the calibration). By varying the number of open HP CFVs in the nozzle bank from two to eight, each of the nine TMWS can be calibrated at seven different volumetric flows. In Stage 5, up to nine of the TMWS are used in parallel to calibrate a MUT.

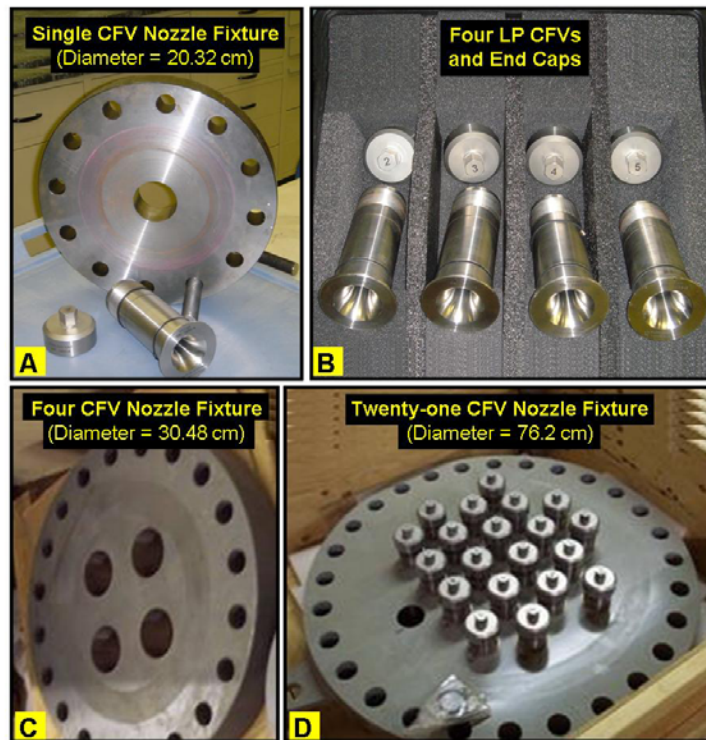


Figure 3. Photographs showing the four LP CFVs with their end caps and the three CFV nozzle fixtures used in Stages 1 through 4.

Based on the five stage process, the NIST NGFCS will be able to offer calibrations for flows ranging from 0.25 m³/s to 9 m³/s at nominal pressures of 7500 kPa and at ambient temperatures. The current expanded uncertainty for these calibrations ranges from 0.25 % to 0.27 % ($k = 2$) depending on flow. Three significant uncertainty sources attributed to the five stage process include 1) the reproducibility of calibrating the TMWS against the HP CFVs in Stage 4; 2) interference effects (*i.e.*, cross-talk) attributed to the spacing between multiple CFVs used in a common plenum in Stages 2, 3, and 4; and 3) uncertainty

attributed to the NIST calibration in Stage 1. Efforts are underway to reduce the uncertainty of each of these effects.

THROAT DIAMETERS VALUES OF THE LP, MP, AND HP CFVs

The throat diameters of the four LP CFVs (d_{LP}) are measured to uncertainties better than 0.001 mm at the 95 % confidence level by the Precision Engineering Division at NIST. On the other hand, the throat diameter values of the four MP CFVs (d_{MP}) and eight HP CFVs (d_{HP}) are estimated so that their respective calibration curves match the LP CFV calibration curve. In Table 1, the throat diameters values for all sixteen CFVs are uniquely identified by their serial numbers. These diameters are used in later sections to calculate the discharge coefficients of the corresponding CFVs.

Table 1. Throat diameter (d) values of the LP, MP, and HP CFVs

LP CFVs	d_{LP} (mm)	MP CFVs	d_{MP} (mm)	HP CFVs	d_{HP} (mm)
#2	25.3932	#10	25.3944	#1	25.4123
#3	25.3910	#11	25.3952	#7	25.3822
#4	25.3935	#12	25.3959	#8	25.3804
#5	25.3883	#13	25.3854	#14	25.3958
N/A	N/A	N/A	N/A	#15	25.3870
N/A	N/A	N/A	N/A	#17	25.3789
N/A	N/A	N/A	N/A	#19	25.3921
N/A	N/A	N/A	N/A	#20	25.4006

Using accurate throat diameter values for the four LP CFVs result in measured C_d values that are nearly identical at the same Reynolds number. Consequently, all four LP CFVs can be characterized by a single calibration curve. In a similar manner, the four MP CFVs and the eight HP CFVs can be also be characterized by a single calibration curve.

GAS COMPOSITION

Two different gases, air and natural gas, are used in the five-stage process. The calibrations of the LP, MP, and HP CFVs in Stages 1 through 3 are done in air. The fluid composition of the air is specified in Table 2. The concentration of water vapor (though not listed in the table) is less than 4.1×10^{-3} and its impact on fluid properties is accounted for in the uncertainty budget.

Table 2. Concentration of air used in Stages 1 through 3 [3]

Component	Mole Fraction (%)
Nitrogen	78.0849
Oxygen	20.9478
Argon	0.934
Carbon Dioxide	0.0314
Neon	0.00182

Table 3. Typical range in natural gas concentration at CEESI's low flow facility.

Component	Mole Fraction (%)
Methane	95.18 to 95.94
Ethane	1.5 to 2.3
Propane	0.055 to 0.3
iButane	0.0008 to 0.03
nButane	0.0003 to 0.04
iPentane	0 to 0.01
nPentane	0 to 0.006
C6+	0 to 0.006
Nitrogen	1.4 to 1.8
Carbon Dioxide	0.5 to 0.7
Hydrogen	0.05 to 0.27
Helium	0.03 to 0.04

In Stages 4 and 5 the working fluid is dry pipeline-quality natural gas. Table 3 shows the typical range in the natural gas composition at the CEESI low facility. The concentration of C6+, which includes hexane and other higher hydrocarbons (*i.e.*, heptane, octane, and nonane), can occasionally be as large as 0.006 %, but is usually less than 0.001 %. The low concentration of C6+, together with the high methane concentration (*i.e.*, more than 95 %), enables commonly used thermodynamic models (*e.g.*, AGA 8 [4], GERG [5], Refprop 7 [6], and Refprop 8 [7]) to accurately predict natural gas properties over a wide range of pressures and temperatures. For example, for the mixture composition in Table 3 the compressibility factor predicted by these four models differs by no more than 0.02 % up to pressures of 8500 kPa at ambient temperatures. Moreover, the maximum difference with experimental measurements (discussed below in the section entitled Stage 4: Calibration of the TMWS using the array of HP CFVs) is less than 0.038 %.

THERMODYNAMIC PROPERTIES

In each of the five stages the relevant thermodynamic properties (*i.e.*, density, compressibility factor, sound speed, specific heat ratio, viscosity, etc.) are calculated using the Refprop 7 thermodynamic database [6].¹ The CFV critical flow function (C_S) is a thermodynamic function of the CFV stagnation pressure (P_0) and stagnation temperature (T_0) for a given gas. This parameter corrects for real gas effects in CFV flows. Although Refprop 7 does not directly calculate C_S , the database is used to determine the intermediate thermodynamic variables used in the calculation. A method analogous to Johnson [8] is implemented in the C_S calculation. In particular, C_S is determined by integrating along an adiabat, beginning at P_0 and T_0 until a unity Mach number is reached.

CALIBRATION RESULTS OF FIVE STAGE PROCESS

Stage 1: Calibration of LP CFVs with NIST's Primary Standard

NIST's 26 m³ *PVTt* primary flow standard uses a timed collection technique to measure the LP CFV mass flow (\dot{m}_{PVTt}) to standard uncertainties of 0.045 % [3]. The mass flow is determined by diverting the CFV flow into a collection tank (initially evacuated to approximately 100 Pa) for a measured time interval. Flow is allowed to accumulate in the collection tank until a pressure of approximately one atmosphere (101.325 kPa) is attained. The mass flow is taken to be the difference between the final mass (*i.e.*, after filling) and initial mass (*i.e.*, before filling) in the collection tank. Both the initial and final masses are determined using the pressure-volume-temperature-time (*PVTt*) method [3]. A schematic of the 26 m³ *PVTt* standard along with the LP CFV is shown in Figure 4. The CFV pressure (P) and temperature (T_m)

¹ Future work will use Refprop 8 [7] which became available as we were nearly finished with this project.

tap locations are positioned one and two pipe diameters, respectively, upstream of the nozzle inlet. These quantities are used to calculate the stagnation pressure (P_0) and temperature (T_0) in accordance with ISO 9300 [2]. The discharge coefficient of each of the four LP CFVs is the ratio of the mass flow measured by the $PVTt$ flow standard (\dot{m}_{PVTt}) and the theoretical mass flow (\dot{m}_{th})

$$C_d^{LP} \equiv \frac{\dot{m}_{PVTt}}{\dot{m}_{th}} = \frac{4\dot{m}_{PVTt}\sqrt{R_u T_0}}{\pi d^2 P_0 C_s \sqrt{\mathcal{M}}} \quad (1)$$

where d is the nozzle throat diameter of the LP CFV given in Table 1, \mathcal{M} is the mixture molar mass, $R_u = 8314.472 \text{ J/kmol}\cdot\text{K}$ is the universal gas constant, and the theoretical mass flow is

$$\dot{m}_{th} = \frac{\pi d^2 P_0 C_s \sqrt{\mathcal{M}}}{4\sqrt{R_u T_0}} \quad (2)$$

based on one-dimensional isentropic flow theory [9]. In this work the Reynolds number is calculated by

$$Re \equiv \frac{4\dot{m}_{th}}{\pi \mu_0 d} = \frac{P_0 d C_s \sqrt{\mathcal{M}}}{\mu_0 \sqrt{R_u T_0}}. \quad (3)$$

where μ_0 is the viscosity evaluated at P_0 and T_0 .

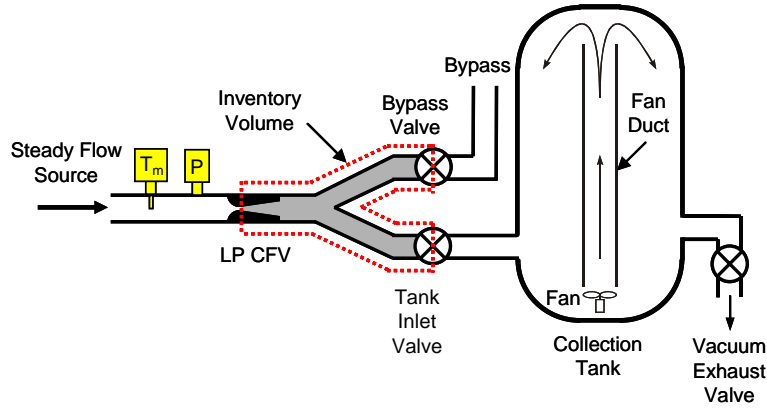


Figure 4. Schematic of the NIST 26 m³ $PVTt$ Primary Flow Standard

Figure 5 shows the calibration data for all four LP CFVs plotted versus the logarithm of the Reynolds number. The figure includes the results of the MP and HP CFVs so that general trends for all three stages of CFV calibration data (*i.e.*, Stages 1, 2, and 3) can be observed together. Also included in Fig. 5 are the theoretically predicted C_d values for commonly used laminar (.....) [10] and turbulent (----) [10] flow models. As expected, the portion of the calibration data below $Re < 10^6$ closely follows the laminar flow model. However, at higher Reynolds numbers the data fall slightly below the currently accepted turbulent flow model. The difference is less than 0.1 % and is well within the expected uncertainty of the turbulent flow model.

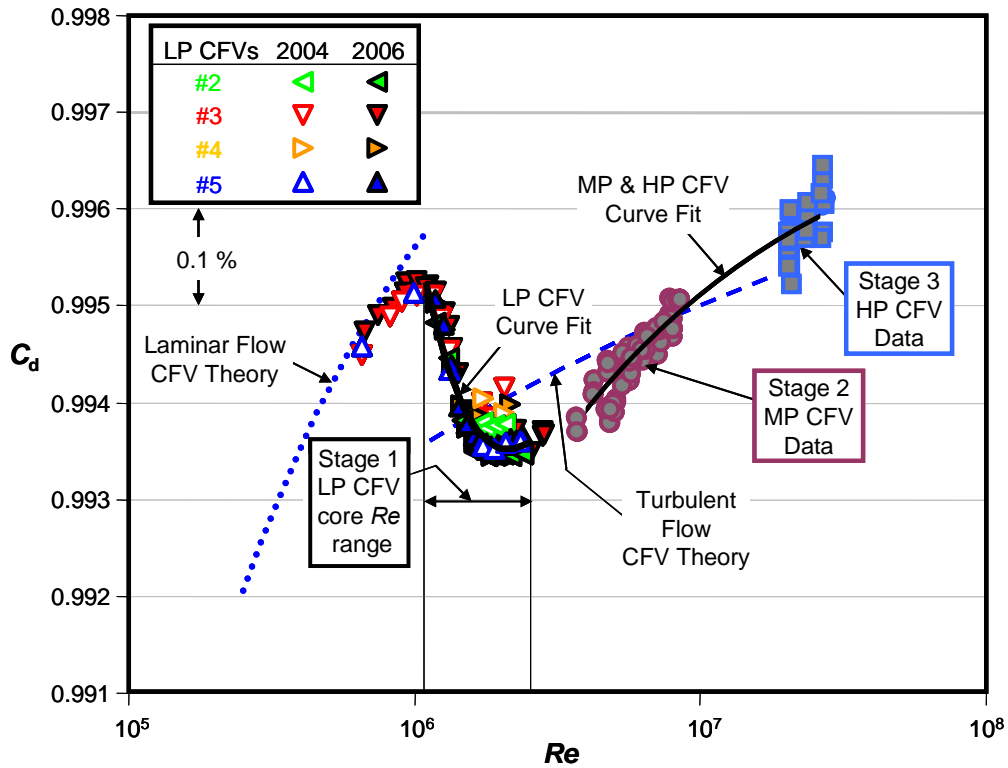


Figure 5. Calibration data for the LP, MP, and HP CFVs.

The LP CFV data shown in the figure incorporate two different $PVTt$ calibrations, the first in 2004, and the second two years later in 2006. In both sets of calibration data the four LP CFVs are depicted by triangles having four different orientations. Open triangles are used for the 2004 dataset (i.e., \triangleleft - CFV #2; ∇ - CFV #3; \triangleright - CFV #4; \triangle - CFV #5) while closed triangles are used for the 2006 dataset (i.e., \blacktriangleleft - CFV #2; \blacktriangledown - CFV #3; \blacktriangleright - CFV #4; \blacktriangle - CFV #5). For clarity, this nomenclature is also denoted in the legend of Fig. 5. Each data point in the figure is the average of a minimum of four repeated $PVTt$ flow measurements at the same nominal flow. In general, the standard deviation of the four (or more in some cases) repeated flow measurements is 0.006 %.

Table 4. Calibration Coefficients for the LP CFVs (Eq. 4), MP CFVs (Eq. 6), and HP CFVs (Eq. 8), and the Reynolds number range where the fit is valid.

CFVs	Reynolds No. Range		Calibration Coefficients		
	Re_{MIN}	Re_{MAX}	b_0	b_1	b_2
LP CFVs	1.1×10^6	2.4×10^6	1.101	-3.917	35.683
MP CFVs	3.7×10^6	8.6×10^6	1.0003	-0.1323	0
HP CFVs	2.0×10^7	2.75×10^7	1.0003	-0.1323	0

All four LP CFVs were calibrated over the core Reynolds number range extending from 1.1×10^6 to 2.4×10^6 . The data within the core Reynolds number range is used in Stage 2 when the array of LP CFVs is used to calibrate the MP CFVs. The Reynolds numbers values outside this core region were obtained primarily to ensure that the data followed the expected theoretical trends in the laminar and turbulent flow regimes. Within the core region, C_d values were measured at no less than 11 equally spaced Re to capture the changes in concavity that occur attributed to transition from laminar to turbulent flow. Considering that the core data includes four different LP CFVs, each calibrated twice two years apart, and

that the data are entirely in the transitional flow regime, the tight overlap between the data is remarkable. As indicated in the figure, the data in the core region for all four LP CFVs can be represented by a single calibration curve

$$C_{d,FIT}^{LP} = b_0 + b_1 Re^{-1/5} + b_2 Re^{-2/5} \quad (4)$$

where the coefficients b_0 , b_1 , and b_2 are given in Table 4, and the standard deviation of the curve fit residuals is 0.018 %. The curve fit coefficients for the MP and HP CFVs are also included in Table 4. The data shown in Fig. 5 are in good agreement with CFV measurements done at other national metrology institutes. In particular, the data agreed to better than 0.05 % with data from PTB (flowing natural gas) and with LADG-LNE (flowing air) [11].

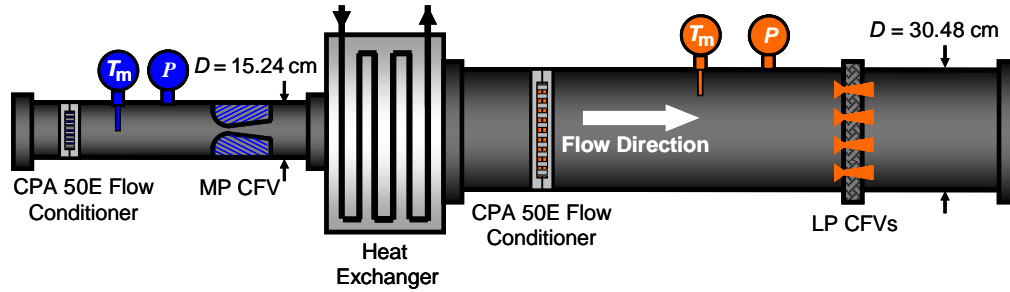


Figure 6. Schematic showing the setup for the Stage 2 calibration of the MP CFV using four LP CFVs calibrated in Stage 1 (figure not drawn to scale).

Stage 2: Calibration of the MP CFVs using the four LP CFVs

In Stage 2, the four LP CFVs calibrated in Stage 1 are combined in parallel and used to calibrate the four MP CFV, one at a time. The calibration setup is shown in Fig. 6. Both the downstream LP CFVs and the upstream MP CFV have a perforated plate flow conditioner installed upstream of their respective pressure and temperature instrumentation. A heat exchanger is used to bring the cold jet exiting the MP CFV back to room temperature conditions (*i.e.*, approximately 25 C) before the flow is measured by the array of four LP CFVs. Based on mass conservation the discharge coefficient of the upstream MP CFV is

$$C_d^{MP} \equiv \left[\frac{\dot{m}}{\dot{m}_{th}} \right]_{MP} = \sqrt{\frac{T_{0,MP}}{T_{0,LP}}} \left(\frac{P_{0,LP} C_{s,LP}}{P_{0,MP} C_{s,MP}} \right) \sum_{n=1}^4 \left(\frac{d_{LP,n}^2}{d_{MP}^2} \right) C_{d,n}^{LP} \quad (5)$$

where $C_{d,n}^{LP}$ is the fitted discharge coefficient of the n^{th} LP CFV calculated via Eq. 4. Mass storage effects² are not considered in Eq. 5, but are taken into account in the uncertainty budget.

For all four MP CFVs, the discharge coefficient is measured at a minimum of five flows on two different occasions. The calibration results are depicted in Fig. 5 (previously shown) where the symbol (●) represents the results of all five MP CFVs. This data set includes a total of 77 points and spans a Reynolds number range from 3.7×10^6 to 8.6×10^6 . Unlike the LP CFV data, the MP CFV data are entirely within the turbulent flow regime. Moreover, the entire MP CFV data set can be fit to a single calibration curve

$$C_{d,FIT}^{MP} = b_0 + b_1 Re^{-1/5} \quad (6)$$

where the coefficients b_0 and b_1 are given in Table 4. Considering that the data correspond to five different CFVs, the small degree of scatter in the data is remarkable. The standard deviation of the curve

² Mass storage or line packing effects are related to temporal changes in the gas density in the piping volume between the single, upstream MP CFV and the four downstream LP CFVs.

fit residuals is only 0.017 %. Perhaps more remarkable is that the same curve fit is also used for the eight HP CFVs.

Stage 3: Calibration of the HP CFVs using the four MP CFVs

In Stage 3 the four MP CFVs are used in parallel to calibrate a total of eight HP CFVs, one at a time, in dry air. The calibration setup is similar to the Stage 2 setup shown in Fig. 6, but in this case a single HP CFV is positioned upstream of the four MP CFVs configured in parallel. The discharge coefficient of any one of the HP CFVs is

$$C_d^{HP} \equiv \left[\frac{\dot{m}}{\dot{m}_{th}} \right]_{HP} = \sqrt{\frac{T_{0,HP}}{T_{0,MP}}} \left(\frac{P_{0,MP} C_{s,MP}}{P_{0,HP} C_{s,HP}} \right) \sum_{n=1}^4 \left(\frac{d_{MP,n}^2}{d_{HP}^2} \right) C_{d,n}^{MP} \quad (7)$$

where $C_{d,n}^{MP} = C_{d,FIT}^{MP}(Re_{MP})$ is the MP CFV curve fit given in Eq. 6, and the throat diameters of the MP and HP CFVs are given in Table 1.

The discharge coefficients for all eight HP CFVs are determined at no less than three flows. The data for the eight HP CFVs include a total of 43 points which span a Reynolds number range from 2.0×10^7 to 2.75×10^7 . The data are depicted by the square symbols (■) in Fig.5. All eight HP CFVs fit a single calibration curve

$$C_{d,FIT}^{HP} = b_0 + b_1 Re^{-1/5} \quad (8)$$

where the coefficients b_0 and b_1 are identical to the MP fit as shown in Table 4, and the standard deviation of the curve fit residuals is 0.02%.

Stage 4: Calibration of the TMWS using the array of HP CFVs

In Stage 4 all nine TMWS are individually calibrated in natural gas *at their place of use* and *at their nominal operating conditions*. Each TMWS is calibrated against the HP CFVs that were calibrated in air in Stage 3. At these high Reynolds numbers (*i.e.*, $Re > 25 \times 10^6$), the air-based calibration can be applied to nozzles flowing natural gas by accounting for real gas effects via the critical flow function, and by matching the Reynolds number [11]. Because the viscosity of natural gas is less than dry air, matching the Reynolds number requires that P_0 in the natural gas flow be approximately 20 % lower than its value in dry air.

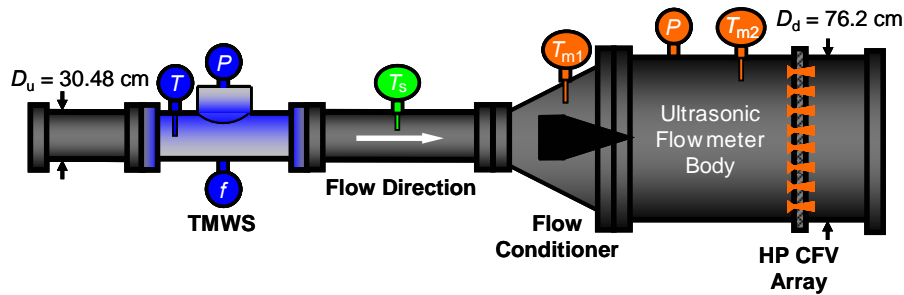


Figure 7. Schematic showing the setup for the Stage 4 calibration of the TMWS using the array of HP CFVs calibrated in Stage 3 (*not drawn to scale*).

The TMWS were calibrated against the HP CFVs on two occasions, once in May 2006, and again in June 2007. A schematic showing the calibration setup of a single TMWS is shown in Fig 7. The flow conditioner installed upstream of the HP CFVs reduces jetting effects and inhibits stratification as the flow transitions from the smaller diameter piping $D_u = 30.48$ cm (12 inch) to the larger diameter piping $D_d = 76.2$ cm (30 inch). Figure 8A is an internal view of the flow conditioner mounted in the pipeline. The average

temperature upstream of the HP CFVs is measured at two cross-sections,³ just before the HP CFV inlet, and two pipe diameters (D_d) upstream of the inlet. Both of these cross sectional temperatures, T_{m1} and T_{m2} , are determined by averaging the readings of 10 RTDs (*i.e.*, resistance temperature device) mounted at equal distances around the circumference of the pipe. The lengths of the RTDs vary so that their penetration depth into the flow stream ranges from 5 cm (*i.e.*, near the pipe wall) to 36 cm (*i.e.*, near the pipe centerline). In this way the temperature is sampled at multiple radii across the cross section. Differences between T_{m1} and T_{m2} are used to estimate the spatial sampling error in the temperature measurement. The locations of the two temperature measurements relative to the HP CFV array are shown in Fig. 8B, and the configuration of the 10 RTDs used to measure T_{m2} is shown in Fig. 8C. Figure 8D shows a picture of the HP CFV array viewed from inside the piping.

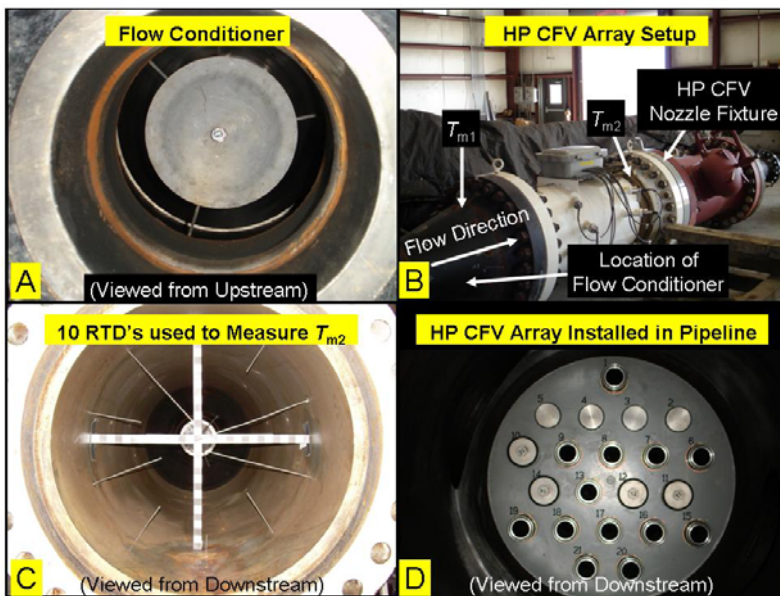


Figure 8. Photographs showing internal view of the flow conditioner upstream of the of HP CFV array (A), an external view of HP CFV array (B), configuration of the 10 RTDs installed in pipeline to measure T_{m2} (C), and an internal view of the HP CFV nozzle fixture installed in pipeline (D).

In both the May 2006 and June 2007 tests an industrial-grade gas chromatograph (GC) was used to measure the natural gas composition. The GC reported the gas composition in the pipeline at five minute intervals. Multiple measurements are needed since the gas composition entering the custody transfer station can change during the calibration cycle. NIST validated the GC composition measurements using two methods. Gas samples collected during the calibration process were analyzed 1) using a laboratory grade gas chromatograph at NIST and 2) by extrapolating densimeter measurements made at NIST to low pressures (*i.e.*, the ideal gas limit) to determine the molar mass (\mathcal{M}). The densimeter measurements were made by McLinden using the two-sinker densimeter described in [12]. The expanded uncertainties (*i.e.*, $k = 2$) of the molar mass from each technique are 0.02 % and 0.009 %, respectively. Moreover, the differences between the molar mass values determined by NIST measurements and the value determined by the industrial GC were 0.01 % and 0.023 %, respectively. The good agreement of these independent measurements demonstrated the reliability of the industrial GC. However, in future work NIST will supply a GC at the lowa flow facility to determine the composition.

The low pressure densimeter measurements (used to determine \mathcal{M}) were repeated at higher pressures (*i.e.*, 6500 kPa to 8500 kPa) and used to determine the compressibility factor (Z). In particular, the compressibility factor is determined using the equation of state ($Z = P\mathcal{M}/\rho R_u T$) where the density (ρ), pressure (P), and temperature (T) are determined respectively from the high pressure densimeter

³ The second temperature measurement (T_{m2}) was added for the Nov. 2007 test.

measurements, and from auxiliary instrumentation used to measure pressure and temperature. Subsequently, the measured Z values are used to determine the uncertainty of the Refprop 7 database at 7500 kPa and 295 K (*i.e.*, the nominal pressure and temperature at the low flow facility) for natural gas mixtures with compositions consistent with Table 1. This uncertainty consists of three components including 1) the standard uncertainty of the measured Z value (0.006 %) ⁴, 2) the offset between the measured and predicted Z at 7500 kPa and 295 K (*i.e.*, assumed to be rectangular distribution, 0.022%), and 3) sensitivity of Z (predicted by Refprop 7) to uncertainty in the gas composition (0.008 %). The root-sum-square of these three components multiplied by a coverage factor of two is the expanded uncertainty Z values predicted by Refprop 7 (0.048 %).

Each of the nine TMWS is calibrated at seven flows ranging from 0.25 m³/s (3.2 × 10⁴ acfh) to 1.0 m³/s (1.3 × 10⁵ acfh) at a nominal pressure of 7500 kPa and at ambient temperatures. We begin by calibrating each of the nine TMWS at the lowest flow with two open HP CFVs. For each higher flow an additional HP CFV is opened until all eight HP CFVs are opened at the maximum flow. At each flow, the measurements are repeated a minimum of three times. The calibration performance of each TMWS is given by its K -factor ($K \equiv f/q_{\text{TMWS}}$), a ratio of the measured frequency to the volumetric flow. When the volumetric flow is determined by the HP CFV array the expression for K -factor is

$$K \equiv \frac{f}{q_{\text{TMWS}}} = \frac{f}{\frac{1}{\rho_{\text{TMWS}}} \sum_{n=1}^{N_4} (\dot{m}_{\text{th},n} C_{\text{d},n})_{\text{HP}}} \quad (9)$$

where N_4 equals the number of open HP CFVs; $\rho_{\text{TMWS}} = [P\mathcal{M}/ZR_uT]_{\text{TMWS}}$ is the density of natural gas at the TMWS where $Z = Z(P, T, x_k)$ is the compressibility factor and $\mathcal{M} = \sum x_k M_k$ is the mixture molar mass – a linear summation of the product the mole fraction (x_k) and species molar mass (M_k). The theoretical mass flow of the n^{th} HP CFV ($\dot{m}_{\text{th},n}^{\text{HP}}$) is determined using an expression analogous to Eq. 2, and the HP CFV discharge coefficient ($C_{\text{d},n}^{\text{HP}}$) is determined via the calibration curve fit given in Eq. 8. Similar to Stages 2 and 3, line pack effects are not accounted for in the expression for K -factor, but they are included in the uncertainty budget.

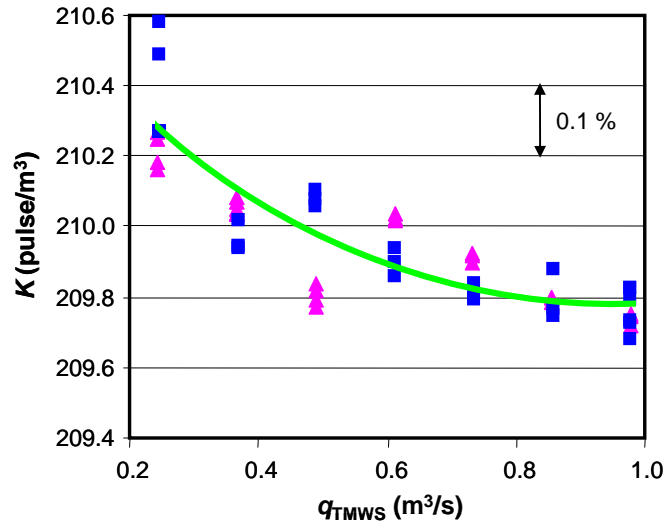


Figure 9. K -factor calibration curve (—) for a typical TMWS plotted versus volumetric flow where the squares (■) are the May 2006 data and the triangles (▲) are the June 2007 data.

⁴ This uncertainty includes contributions from the molecular mass determination, the density measured via the densimeter, the universal gas constant, and pressure and temperature measurements.

Figure 9 shows typical calibration data for one of the nine TMWS where the K -factor is plotted as a function of the volumetric flow. The plot includes the May 2006 data (■), the June 2007 data (▲), and a third degree polynomial curve fit of both sets of data (—). The calibration data for all nine TMWS have the same general shape, consisting of a curve with a downward slope that flattens with increasing flow. In general, the May 2006 and June 2007 data sets are in good agreement. The K -factors of the two data sets overlapped at several flows, and the average difference between the data sets is well within the 0.24 % uncertainty ($k = 2$). The repeatability (*i.e.*, standard deviation of three or more points taken sequentially at the same nominal flow) of the May 2006 and June 2007 data sets was typically 0.02 % and 0.01 %, respectively, at all but the lowest flows. The reproducibility between the two data sets (*i.e.*, standard deviation of the K -factor residuals of the May 2006 and June 2007 data) is 0.056 %.

Stage 5: Calibration of a MUT using the TMWS

The volumetric flow of a MUT is calibrated against the array of NIST-traceable TMWS shown previously in Fig. 1. The expression for volumetric flow at the MUT is

$$q_{MUT} = \sum_{n=1}^{N_5} \left(\frac{\rho_{TMWS,n}}{\rho_{MUT}} \right) \left(\frac{f_n}{K_{TMWS,n}} \right) \quad (10)$$

where N_5 specifies how many of the nine TMWS are used in the calibration, and the ratio $f_n/K_{TMWS,n}$ is the volumetric flow of the n^{th} TMWS. The frequency (f_n) is measured at each TMWS and the K -factor is determined from the Stage 4 calibration. The densities are determined at the measured pressures, temperatures, and gas composition using the Refprop 7 database. Pressure and temperature measurements are made at the MUT and at each TMWS while the gas composition is measured just upstream of the TMWS using an industrial GC.

UNCERTAINTY ANALYSIS OF THE FIVE STAGE PROCESS

The method of propagation of uncertainty [13] as specified in the GUM [14] is used to determine the uncertainty of the five-stage process. The uncertainty is propagated through the five calibration equations governing each of the five stages. These five equations are Eqs. 1, 5, 7, 9, and 10, respectively. The analysis begins with Stage 1 and proceeds sequentially to Stage 5. The results indicate that the expanded uncertainty (*i.e.*, $k = 2$) of a MUT ranges from 0.25 % to 0.27 % over volumetric flows extending from 9 m³/s to 0.25 m³/s at a nominal pressure of 7500 kPa and at ambient temperatures.

The results of the uncertainty analysis for a volumetric flow of $q_{MUT} = 2.25$ m³/s are summarized in the bar graph shown in Fig. 10. Each of the rectangles indicates the uncertainty contribution of the stage it represents. The number written just above each rectangle is the standard uncertainty (*i.e.*, $k = 1$) of that stage. The sum of all five rectangles is 100 % and the root-sum-square of the standard uncertainties multiplied by a coverage factor of two is the expanded uncertainty (*i.e.*, 0.25 %) of the MUT.

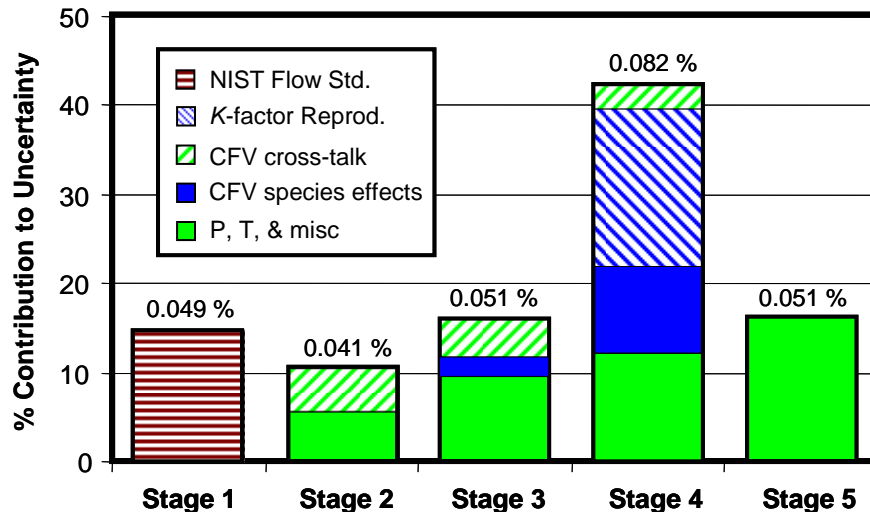


Figure 10. The standard uncertainty and the percent contribution to the total uncertainty of each stage for $q_{MUT} = 2.25 \text{ m}^3/\text{s}$. (The height of each rectangle indicates the uncertainty contribution in percent for the corresponding stage.)

The legend in Fig. 10 shows the five different shading patterns used in the bar graph. The three lined shading patterns (*i.e.*, , , ) denote uncertainty components that NIST is currently working to reduce. These include the uncertainty introduced in Stage 1 corresponding to the NIST flow standard () , the uncertainty introduced in Stage 4 attributed to the reproducibility of the TMWS *K*-factors () , and the uncertainty introduced in Stages 2, 3, and 4 attributed to cross-talk (*i.e.*, interference effects) between the CFVs mounted in a common plenum () . The CFV interference effects will be reduced by increasing the spacing between the CFVs used in parallel. The *K*-factor reproducibility is currently based on only two calibrations. We anticipate lower values in the future as repeated calibrations provide a larger data set to more accurately determine the long term random effects and flowmeter drift. Lastly, NIST is currently working to reduce the uncertainty of the NIST flow standard used in Stage 1.

The two solid shading patterns (*i.e.*,  and ) in Stages 2, 3, 4, and 5 include multiple uncertainty sources that have been grouped together. The first pattern of solid shading () includes uncertainty components attributed to pressure and temperature measurements, line pack effects, and various other sources. A detailed listing of the individual uncertainty components contained in these groupings is beyond the scope of this document, but is provided in [15, 16].

The second pattern of solid shading () is attributed to CFV species effects. CFV species effects include uncertainty contributions from the following four thermodynamic properties: C_s for air in Stage 3, and C_s , Z , and \mathcal{M} for natural gas in Stage 4. The cause of this uncertainty is twofold. First, the uncertainty attributed to C_s in Stages 3 and 4 is a consequence of calibrating the HP CFVs in air, but applying the calibration in natural gas. Second, the Stage 4 uncertainty attributed to Z and \mathcal{M} results because the density of the natural gas is required to convert from the mass flow predicted by the HP CFVs to volumetric flow needed for the TMWS calibration (see Eq. 9). The uncertainties of the Refprop 7 database used to predict Z , and the GC measurements used to determine \mathcal{M} have already been reduced via the calibration processes explained Stage 4. Consequently, the uncertainty attributed to CFV species effects is not expected to decrease. This uncertainty is intrinsic to using air-calibrated CFVs to calibrate the TMWS in natural gas.

SUMMARY AND CONCLUSIONS

This manuscript documents the results and uncertainty of a five-stage scale-up process that establishes traceability between NIST's $26 \text{ m}^3 \text{ PVTt}$ primary flow standard (*i.e.*, applicable to low pressure air) and CEESI's Iowa natural gas flow facility. The traceability path described, combined with NIST metrological control procedures, establishes U.S. national standards for calibration of flowmeters used in custody transfer of high pressure natural gas. When completed, the national standard will provide internationally recognized flowmeter calibrations to the natural gas industry. The flow range will range from $0.25 \text{ m}^3/\text{s}$ ($3.2 \times 10^4 \text{ acfh}$) to $9 \text{ m}^3/\text{s}$ ($1.1 \times 10^6 \text{ acfh}$) at a nominal pressure of 7500 kPa and at ambient temperatures. The measurement uncertainty of these calibrations will range from 0.25 % to 0.27 % (at a 95 % confidence level) depending on flow. Work has begun to reduce the uncertainty to 0.20 % while simultaneously extending the flow range down to $0.1 \text{ m}^3/\text{s}$ ($1.3 \times 10^4 \text{ acfh}$). NIST and CEESI will establish a Cooperative Research and Development Agreement (CRADA) through which joint research efforts will be conducted to advance flow measurement capabilities in natural gas flows with the objective of improving the realization of these standards.

REFERENCES

- [1] International Organization for Standardization, "General requirements for the competence of testing and calibration laboratories," ISO/IEC FDIS 17025:2005(E).
- [2] International Standards Organization (ISO), *Measurement of Gas Flow by Means of Critical Flow Venturi Nozzles*, ISO 9300:2005(E).

-
- [3] Johnson, A. N., Wright, J. D., *Gas Flowmeter Calibrations with the 26 m³ PVTt Standard*, NIST Special Publication 250-1046, National Institute of Standards and Technology, Gaithersburg, MD, (2006).
- [4] American Gas Association (AGA); *Compressibility Factor of Natural Gas and Other Related Hydrocarbon Gases*, AGA Transmission Measurement Committee Report No. 8 (AGA8), 1994.
- [5] Kunz, O., Klimeck, R., Wagner, W., and Jaeschke, M. The GERG-2004 Wide-Range Equation of State for Natural Gases and Other Mixtures, GERG TM15, 2007.
- [6] Lemmon, E. W., McLinden, M. O., and Huber, M. L., *NIST Standard Reference Database 23: Reference Fluid Thermodynamic and Transport Properties-REFPROP Version 7.0* National Institute of Standards and Technology, Standard Reference Data Program, Gaithersburg, 2002.
- [7] Lemmon, E. W., Huber, M. L., and McLinden, M. O. *NIST Standard Reference Database 23: Reference Fluid Thermodynamic and Transport Properties-REFPROP*, Version 8.0 National Institute of Standards and Technology, Standard Reference Data Program, Gaithersburg, 2007.
- [8] Johnson, R. C., *Calculations of Real-Gas Effects in Flow Through Critical Nozzles*, Journal of Basic Engineering, September 1964, pp. 519.
- [9] John, J. E., Gas Dynamics, Allyn and Bacon, Inc, 2nd edition, Boston, 1984.
- [10] Mickan, B., Kramer, R., Dopheide, D., *Determination of Discharge Coefficient of Critical Nozzles Based on Their Geometry and The Theory of Laminar and Turbulent Boundary Layers*, Proceedings of the International Symposium on Fluid Flow Measurement, Queretaro, Mexico, (2006).
- [11] Mickan, B., Kramer, R., Dopheide, D., Hotze, H., Hinze, H., Johnson, A, Wright, J., Vallet, J.-P., *Comparisons by PTB, NIST, and LNE-LADG, in Air and Natural Gas with Critical Venturi Nozzles Agree within 0.05 %*, Proceedings of the International Symposium on Fluid Flow Measurement, Queretaro, Mexico, (2006).
- [12] McLinden, M. O., and Loscg-Will, C., *Apparatus for wide-ranging, high-accuracy fluid (p, ρ, T) measurements based on a compact two-sinker densimeter*, J. Chem. Thermodynamics 39 (2007) 507–530.
- [13] Coleman, H. W., and Steele, W. G., *Experimentation and Uncertainty Analysis for Engineers*, John Wiley and Sons, Inc., New York, NY, 1989.
- [14] Taylor, B. N. and Kuyatt C. E., *Guidelines for the Evaluating and Expressing the Uncertainty of NIST Measurement Results*, NIST Technical Note-1297, MD, 1994.
- [15] Johnson, A. N. and Kegel, T., *Uncertainty and Traceability for the CEESI Iowa Natural Gas Facility*, J. Res. Natl. Inst. Stand. Technol. 109, 345-369, (2004).
- [16] Johnson, A. N., *Natural Gas Flow Calibration Service (NGFCS) NIST, Special Publication*, National Institute of Standards and Technology, Gaithersburg, MD, (in. press.).